

Cite this: *Chem. Sci.*, 2019, 10, 497

All publication charges for this article have been paid for by the Royal Society of Chemistry

# MoS<sub>2</sub>-quantum dot triggered reactive oxygen species generation and depletion: responsible for enhanced chemiluminescence†

Xiangnan Dou,<sup>ab</sup> Qiang Zhang,<sup>a</sup> Syed Niaz Ali Shah,<sup>a</sup> Mashooq Khan,<sup>a</sup> Katsumi Uchiyama<sup>b</sup> and Jin-Ming Lin<sup>\*a</sup>

Reactive oxygen species (ROS) generation is of intense interest because of its crucial role in many fields. Here we demonstrate that MoS<sub>2</sub>-QDs exhibit a promising capability for the generation of reactive oxygen species, which leads to enhanced chemiluminescence. We discovered that the unique performance is due to hydroxyl radical activation increasing the active catalytic sites on molybdenum sulphide quantum dots (MoS<sub>2</sub>-QDs). The reactive oxygen species, such as hydroxyl radicals (<sup>•</sup>OH), superoxide radicals (<sup>•</sup>O<sub>2</sub><sup>−</sup>) and singlet oxygen (<sup>1</sup>O<sub>2</sub>) have been efficiently generated from H<sub>2</sub>O<sub>2</sub> solution in alkaline conditions. In particular, the maximum <sup>•</sup>OH yield was enhanced significantly (9.18 times) compared to the Fe(II)/H<sub>2</sub>O<sub>2</sub> Fenton system under neutral conditions. These findings not only enrich our understanding of the fascinating performance of MoS<sub>2</sub> QDs, but also provide a new pathway for ROS generation in all kinds of pH environment.

Received 7th August 2018  
Accepted 13th October 2018

DOI: 10.1039/c8sc03511c

rsc.li/chemical-science

## Introduction

Reactive oxygen species (ROS) is a collective term for oxygen free radicals and molecules including superoxide radicals (<sup>•</sup>O<sub>2</sub><sup>−</sup>), hydroxyl radicals (<sup>•</sup>OH) and singlet oxygen (<sup>1</sup>O<sub>2</sub>), which possess high reactivity compared to molecular O<sub>2</sub>. Generation of abundant ROS is of immense interest in environmental and biological sciences.<sup>1</sup> To date, the ROS are usually generated using a photocatalytic process *via* light-activated photosensitizers or a chemical process *via* iron-mediated Fenton reaction.<sup>2</sup> However, the photocatalytic process suffers from undesirable bio-damage by ultra-violet (UV) radiation and low reactive oxygen species production. This has restricted the role of photocatalysis for biomedical applications.<sup>3</sup> The Fenton reaction can generate adequate ROS, however, this requires acidic conditions (pH = 3–4). Therefore, alternative reactions and conditions for ROS generation need to be pursued.

Nanoscale molybdenum sulphides (MoS<sub>2</sub>) have gained widespread application in photo-responsive, energy storage and biosensor devices.<sup>4</sup> Besides, MoS<sub>2</sub> has been used as an excellent electro-catalyst for the hydrogen evolution reaction (HER).<sup>5</sup>

However, the performance of molybdenum sulphide-quantum dots (MoS<sub>2</sub>-QDs) toward chemiluminescence (CL) based on ROS generation has not been explored.

Here, we demonstrate the excellent capability of MoS<sub>2</sub>-QDs to generate ROS from hydrogen peroxide in alkaline solution,

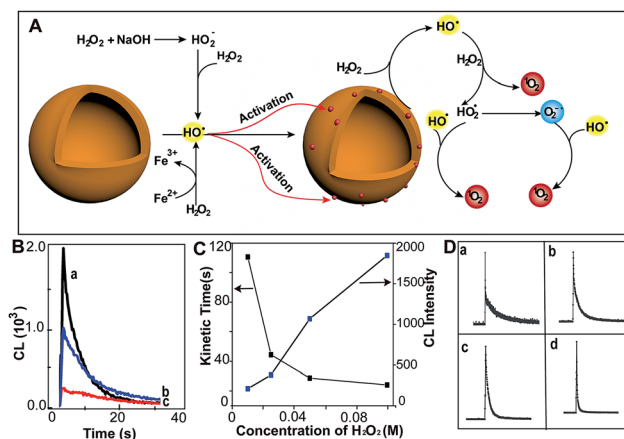


**Fig. 1** MoS<sub>2</sub>-QDs promote the generation of reactive oxygen species and induce chemiluminescence with H<sub>2</sub>O<sub>2</sub> in alkaline conditions. (A) Schematic illustration of ROS generation by MoS<sub>2</sub>-QDs. (B) The CL spectrum of injection order with (a) injection of MoS<sub>2</sub>-QDs into a mixture of H<sub>2</sub>O<sub>2</sub> + NaOH, (b) injection of NaOH into a mixture of H<sub>2</sub>O<sub>2</sub> + MoS<sub>2</sub>-QDs and (c) injection of H<sub>2</sub>O<sub>2</sub> into a mixture of MoS<sub>2</sub>-QDs + NaOH. (C) The dose-dependence of H<sub>2</sub>O<sub>2</sub> concentration on kinetic decay time and CL intensity by injection of MoS<sub>2</sub>-QDs into a H<sub>2</sub>O<sub>2</sub>-NaOH solution. (D) The CL kinetic curve at H<sub>2</sub>O<sub>2</sub> concentrations of (a) 0.01, (b) 0.025, (c) 0.05, and (d) 0.1 M.

<sup>a</sup>Beijing Key Laboratory of Microanalytical Methods and Instrumentation, MOE Key Laboratory of Bioorganic Phosphorus Chemistry & Chemical Biology, Department of Chemistry, Tsinghua University, Beijing, 100084, China. E-mail: jmlin@mail.tsinghua.edu.cn

<sup>b</sup>Department of Applied Chemistry, Graduate School of Urban Environmental Sciences, Tokyo Metropolitan University, Minamioshima, Hachioji, Tokyo 192-0397, Japan

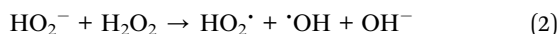
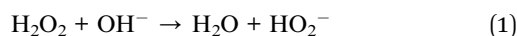
† Electronic supplementary information (ESI) available. See DOI: 10.1039/c8sc03511c

which gives rise to CL emission (Fig. 1A). The hydroxyl radicals ( $\cdot\text{OH}$ ) from intrinsic reactions such as  $\text{H}_2\text{O}_2$  in alkaline medium and the  $\text{Fe(II)}/\text{H}_2\text{O}_2$  Fenton system activate  $\text{MoS}_2$ -QDs and generate active catalytic sites on their surface. These active sites then facilitate the conversion of  $\text{H}_2\text{O}_2$  to generate a sufficient amount of ROS, which leads to a strong CL-emission.

## Results and discussion

The  $\text{MoS}_2$ -QDs were prepared by solvothermal treatment in  $N,N$ -dimethylformamide (DMF), as proposed by Wang *et al.*<sup>6</sup> The  $\text{MoS}_2$ -QDs exhibited an average size of  $\sim 3.7$  nm (Fig. S1, ESI†). The as-prepared product ( $0.9$  mg  $\text{ml}^{-1}$ ) was dispersed in water and a transparent pale-yellow solution was obtained, which exhibited a strong fluorescence emission over a wide range of excitation wavelengths (Fig. S2, ESI†).

The chemiluminescence (CL) was produced by  $\text{MoS}_2$ -QDs and  $\text{H}_2\text{O}_2$ . A stronger CL was obtained with injection of the  $\text{MoS}_2$ -QD suspension into a pre-mixed  $\text{H}_2\text{O}_2/\text{NaOH}$  solution, whereas those with the addition of  $\text{H}_2\text{O}_2$  to  $\text{NaOH}/\text{MoS}_2$ -QDs or with the addition of  $\text{NaOH}$  to  $\text{H}_2\text{O}_2/\text{MoS}_2$ -QDs, exhibited relatively weaker CL-emission (Fig. 1B). We found that the CL was not only correlated to the injection order, but also to the  $\text{NaOH}$  concentration. The CL intensity was found to increase with increasing concentration of  $\text{NaOH}$  and no CL emission was found under acidic or neutral conditions. This was attributed to the remarkable decomposition of  $\text{H}_2\text{O}_2$  in alkaline medium<sup>7</sup> (80% and 15% at  $\text{pH} = 13$  and  $10.5$  respectively) (Fig. S3, ESI†). The results suggested that the decomposition of  $\text{H}_2\text{O}_2$  plays an important role in the enhanced CL-emission with the addition of  $\text{MoS}_2$ -QDs. The hydroxyl radical ( $\cdot\text{OH}$ ) generation from  $\text{H}_2\text{O}_2$  in the presence of base is given in eqn (1) and (2). Peroxyhydroxyl ions ( $\text{HO}_2^-$ ) were formed through the decomposition of  $\text{H}_2\text{O}_2$  in base; then the  $\text{HO}_2^-$  reacted with undissociated  $\text{H}_2\text{O}_2$  molecules to produce hydroperoxide radicals ( $\text{HO}_2\cdot$ ) and  $\cdot\text{OH}$ .<sup>8</sup>



Ouyang *et al.* have reported that intrinsic defects can be generated to activate and increase the number of catalytic sites on  $\text{MoS}_2$ .<sup>9</sup> The  $\cdot\text{OH}$  is a strong oxidizing agent, which has a redox potential of  $2.8$  V,<sup>10</sup> therefore, the production of  $\cdot\text{OH}$  leads to radical attack on the  $\text{MoS}_2$ -QDs and generates defects. This increases the effective catalytic sites of the  $\text{MoS}_2$ -QDs and hence facilitates the further decomposition of  $\text{H}_2\text{O}_2$ . The occurrence of defects was evidenced by the short lifetime of about  $5.2$  ns of the  $\text{MoS}_2$ -QDs (Fig. S4, ESI†). To clarify the role of  $\cdot\text{OH}$  in the strong CL-emission of the  $\text{MoS}_2$ -QD/ $\text{H}_2\text{O}_2$  system, experiments with  $\text{H}_2\text{O}_2$  at different concentrations were performed. We found that the CL-emission intensity of the  $\text{MoS}_2$ -QD/ $\text{H}_2\text{O}_2$  system is dependent on the concentration of  $\text{H}_2\text{O}_2$  (Fig. 1C). With increasing  $[\text{H}_2\text{O}_2]$  from  $0.01$  M to  $0.1$  M, the intensity of CL increased progressively. The CL kinetic decay time was also found to be dependent on the  $\text{H}_2\text{O}_2$  concentration. A flash CL-emission was observed at high  $\text{H}_2\text{O}_2$

concentration ( $0.1$  M), whereas a relatively slower decay was observed at low concentration (Fig. 1D).

Electron Spin Resonance (ESR) spectroscopy was performed to directly examine the generation of  $\cdot\text{OH}$  under different  $\text{H}_2\text{O}_2$  conditions. A larger yield of  $\cdot\text{OH}$  was observed as  $[\text{H}_2\text{O}_2]$  was increased (Fig. 2A(a) and B(a)). This provides clear evidence that activation of the  $\text{MoS}_2$ -QDs is highly dependent on  $\cdot\text{OH}$  formation. No obvious ESR signals for  $\text{DMPO}-\text{OH}$  were observed without  $\text{MoS}_2$ -QDs, while the  $\cdot\text{OH}$  was significantly enhanced in the presence of activated  $\text{MoS}_2$ -QDs at  $[\text{H}_2\text{O}_2] = 0.01$  M in  $\text{NaOH}$  ( $0.1$  M) (Fig. 2A(b)). In addition, we found the signal for  $\text{DMPO}-\text{OH}$  and  $\text{DMPO}-\cdot\text{O}_2^-$  (ref. 11) in the presence of  $\text{MoS}_2$ -QDs is stronger than that in the absence of  $\text{MoS}_2$ -QDs at  $\text{H}_2\text{O}_2 = 0.1$  M in  $\text{NaOH}$  ( $0.1$  M) (Fig. 2B(b)). These results suggest the dependence of  $\cdot\text{OH}$  generation on  $\text{H}_2\text{O}_2$  concentration and the ability of the  $\text{MoS}_2$ -QDs for ROS generation, which leads to the strong CL-emission of the  $\text{MoS}_2$ -QD/ $\text{H}_2\text{O}_2$  system.

Moreover, the UV-vis spectra (Fig. 2C) with nitrotetrazolium blue chloride (NBT) as a superoxide radical ( $\cdot\text{O}_2^-$ ) probe<sup>12</sup> and ESR spectra (Fig. 2D) with 2,2,6,6-tetramethyl-4-piperidine (TEMP) as a singlet oxygen ( $^1\text{O}_2$ ) probe<sup>13</sup> also showed a significant increase in  $\cdot\text{O}_2^-$  and  $^1\text{O}_2$  production in the presence of  $\text{MoS}_2$ -QDs. The generation pathways of  $\cdot\text{O}_2^-$  and  $^1\text{O}_2$  via radical reactions are given in eqn (3)–(7).<sup>14,15</sup> We hypothesized that the active sites induced by  $\cdot\text{OH}$  were responsible for the generation of  $\cdot\text{OH}$ ,  $\cdot\text{O}_2^-$ , and  $^1\text{O}_2$  by facilitating the conversion of  $\text{H}_2\text{O}_2$  into more ROS.

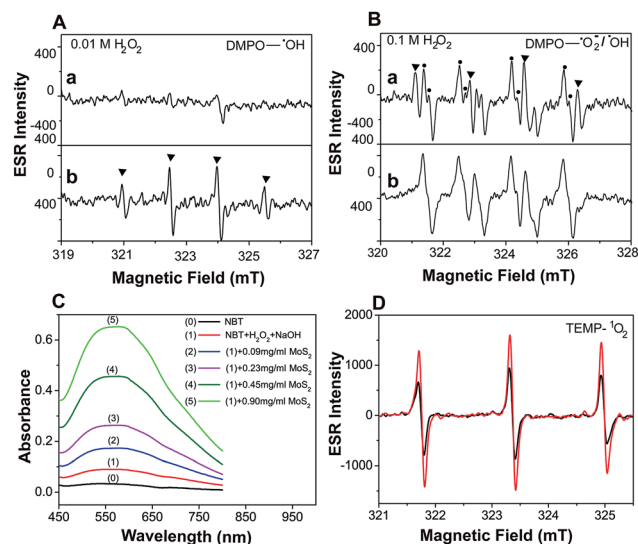
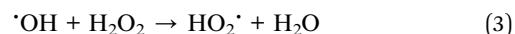
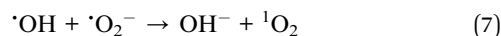
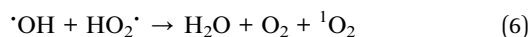
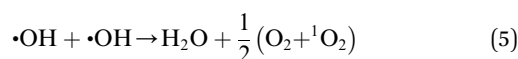
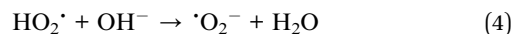


Fig. 2 Evaluation of the enhancement of  $\cdot\text{OH}$ ,  $\cdot\text{O}_2^-$  and  $^1\text{O}_2$  production by  $\text{MoS}_2$ -QDs in the  $\text{H}_2\text{O}_2$ – $\text{NaOH}$  system. (A) ESR spectrum of 5,5-dimethyl-1-pyrroline  $N$ -oxide (DMPO) with  $\cdot\text{OH}$  obtained from  $0.01$  M  $\text{H}_2\text{O}_2$  in  $0.1$  M  $\text{NaOH}$  (a), and the same as the above conditions but with  $\text{MoS}_2$ -QDs (b). (B) ESR spectrum of DMPO with  $\cdot\text{OH}$  or  $\cdot\text{O}_2^-$  obtained from  $0.1$  M  $\text{H}_2\text{O}_2$  in  $0.1$  M  $\text{NaOH}$  (a), and the same as the above conditions but with  $\text{MoS}_2$ -QDs (b). (C) The absorbance of NBT in the  $\text{H}_2\text{O}_2$ – $\text{NaOH}$  system with the addition of  $\text{MoS}_2$ -QDs. (D) ESR spectrum of TEMP with  $^1\text{O}_2$  production from  $\text{H}_2\text{O}_2$ – $\text{NaOH}$  (black) and  $\text{MoS}_2$ -QDs– $\text{H}_2\text{O}_2$ – $\text{NaOH}$  (red).



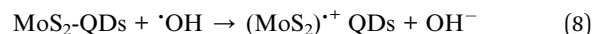


In order to further evaluate the dependence of MoS<sub>2</sub>-QD activation and CL-emission on the generation and concentration of  $\cdot\text{OH}$ , a classic  $\cdot\text{OH}$  generation Fenton system was investigated. We found that, MoS<sub>2</sub>-QDs strongly enhanced the CL-emission of the Fe<sup>2+</sup>/H<sub>2</sub>O<sub>2</sub> system. It was striking that equivalent CL-emission was produced under both neutral and acidic conditions (Fig. 3A). Besides,  $\cdot\text{OH}$  generation was significantly accelerated and compared to the Fe<sup>2+</sup>/H<sub>2</sub>O<sub>2</sub> system, a 9.18 times greater yield of  $\cdot\text{OH}$  was observed (Fig. 3B). These results confirmed the hypothesis of ROS generation through  $\cdot\text{OH}$ -activated MoS<sub>2</sub>-QDs.

To further verify the generation of  $\cdot\text{OH}$ , the Fenton-oxidation of tetramethylbenzidine (TMB) was introduced, which is known to be oxidized by  $\cdot\text{OH}$ .<sup>16</sup> In the absence of MoS<sub>2</sub>-QDs, TMB was oxidized slowly and reached a maximum absorbance intensity ( $\lambda_{\text{max}} = 652 \text{ nm}$ ) after 60 s. Nevertheless, in presence of MoS<sub>2</sub>-QDs, a rapid strong absorbance at 652 nm was observed (Fig. S5, ESI†), indicating a rapid formation of the bluish oxidized TMB because of  $\cdot\text{OH}$  being generated in large amounts. This confirmed that MoS<sub>2</sub>-QD driven Fenton reaction can effectively produce  $\cdot\text{OH}$ .

The generation of  $\cdot\text{OH}$  can effectively degrade organic contaminants.<sup>17</sup> Therefore, phenol, pyrocatechol, rhodamine B (RhB) and methylene blue (MB) were used to find the degradation efficiency and fate of  $\cdot\text{OH}$  in the Fenton (Fe<sup>2+</sup>/H<sub>2</sub>O<sub>2</sub>) and MoS<sub>2</sub>-QD supported Fenton system. Phenolic compound concentrations were measured by using 4-aminoantipyrine for the colorimetric determination.<sup>18</sup> As expected, a significant decrease of phenol and pyrocatechol (Fig. S6, ESI†) was

observed when phenol or pyrocatechol were incubated with the MoS<sub>2</sub>-QD supported Fe<sup>2+</sup>/H<sub>2</sub>O<sub>2</sub> system as compared to the traditional Fe<sup>2+</sup>/H<sub>2</sub>O<sub>2</sub> Fenton system, indicating a higher degradation efficiency for phenolic compounds with the Fe<sup>2+</sup>/H<sub>2</sub>O<sub>2</sub>-MoS<sub>2</sub>-QD system. In addition, the degradation of RhB and MB has been detected by the UV-visible method. In the presence of MoS<sub>2</sub>-QDs, MoS<sub>2</sub>-QDs were found to significantly inhibit both RhB and MB degradation efficiency (Fig. 4). Moreover, the presence of MoS<sub>2</sub>-QDs showed a more negative influence on MB degradation, inhibiting the efficiency of MB degradation by 72%, as well as that of RhB degradation efficiency by 8%. This difference towards RhB and MB degradation is probably attributable to the lower reactivity of MB compared to RhB in the Fe<sup>2+</sup>/H<sub>2</sub>O<sub>2</sub>-MoS<sub>2</sub>-QD system, because of significant structural differences between the two different organic fractions (RhB and MB). It has been found previously that  $\cdot\text{OH}$  could be consumed by injection of holes into semiconductor nano-materials.<sup>19</sup> The selective degradation of phenolic compounds as compared to RhB and MB is probably due to the higher reaction rate of  $\cdot\text{OH}$  with phenolic compounds ( $k \approx 10^{10} \text{ M}^{-1} \text{ s}^{-1}$ ),<sup>20</sup> which makes phenolic compounds more competitive for reacting with  $\cdot\text{OH}$  rather than MoS<sub>2</sub>-QDs in the degradation process. In contrast,  $\cdot\text{OH}$  reacts with MoS<sub>2</sub>-QDs preferentially rather than the aromatic heterocyclic compounds, such as RhB and MB, due to the one order of magnitude lower rate ( $k \approx 10^9 \text{ M}^{-1} \text{ s}^{-1}$ ).<sup>21</sup> These results strongly indicated that a rapid reaction of MoS<sub>2</sub>-QDs with  $\cdot\text{OH}$  (and  $\text{O}_2^{\cdot-}$ ) forming hole-injection ((MoS<sub>2</sub>)<sup>+</sup> QDs) and electron-injection ((MoS<sub>2</sub>)<sup>-</sup> QDs) species (eqn (8) and (9)) occurred.



The annihilation of (MoS<sub>2</sub>)<sup>+</sup> and (MoS<sub>2</sub>)<sup>-</sup> resulted in energy release in the form of CL emission,<sup>22</sup> which has been clarified

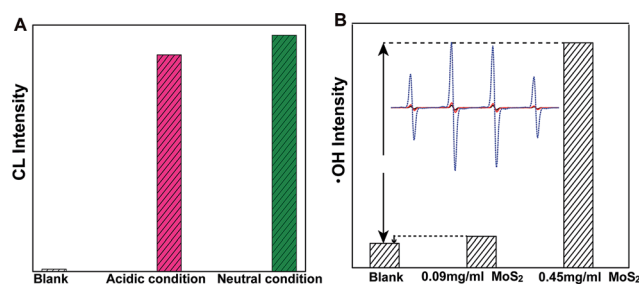


Fig. 3 Enhancement of chemiluminescence and hydroxyl radical ( $\cdot\text{OH}$ ) production by MoS<sub>2</sub>-QDs in the Fe<sup>2+</sup>-H<sub>2</sub>O<sub>2</sub> system (A) the chemiluminescence of Fe<sup>2+</sup>-H<sub>2</sub>O<sub>2</sub> (blank); and the CL produced by the addition of MoS<sub>2</sub>-QDs to the Fe<sup>2+</sup>-H<sub>2</sub>O<sub>2</sub> system under acidic (pH = 3.7) and neutral conditions. (B) The hydroxyl radicals generated from Fe<sup>2+</sup>-H<sub>2</sub>O<sub>2</sub> (blank) and from the addition of MoS<sub>2</sub>-QDs with a concentrations of 0.09 mg ml<sup>-1</sup> and 0.45 mg ml<sup>-1</sup>. The inset in panel B is the ESR spectrum of DMPO with  $\cdot\text{OH}$  generated from Fe<sup>2+</sup>-H<sub>2</sub>O<sub>2</sub> (black) and with the addition of MoS<sub>2</sub>-QDs with concentrations of 0.09 mg ml<sup>-1</sup> (red) and 0.45 mg ml<sup>-1</sup> (blue).

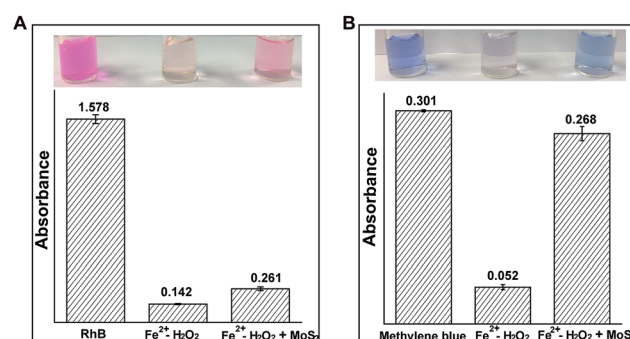


Fig. 4 The influence of MoS<sub>2</sub>-QDs on organic contaminant degradation in the Fe<sup>2+</sup>-H<sub>2</sub>O<sub>2</sub> Fenton system. (A) The absorbance of rhodamine B at 554 nm in the Fe<sup>2+</sup>-H<sub>2</sub>O<sub>2</sub> and Fe<sup>2+</sup>-H<sub>2</sub>O<sub>2</sub> + MoS<sub>2</sub>-QD systems; (B) the absorbance of methylene blue at 626 nm in the Fe<sup>2+</sup>-H<sub>2</sub>O<sub>2</sub> and Fe<sup>2+</sup>-H<sub>2</sub>O<sub>2</sub> + MoS<sub>2</sub>-QD systems. The solution conditions were 0.01 M H<sub>2</sub>O<sub>2</sub>, 0.45 mg ml<sup>-1</sup> MoS<sub>2</sub>-QDs, 1 mM Fe<sup>2+</sup>, 5 μg ml<sup>-1</sup> RhB and 5 μg ml<sup>-1</sup> MB.



through a CL-emission spectrum. The CL emission spectrum was centered at 490 nm and 550 nm, which may contain overlap of  $^1\text{O}_2$  and  $\text{MoS}_2$  emission<sup>23</sup> (Fig. S7, ESI†). To verify that this emission was from the recombination of  $(\text{MoS}_2)^{+\bullet}$  and  $(\text{MoS}_2)^{-\bullet}$  and not from the overlap of  $^1\text{O}_2$  and  $\text{MoS}_2$ -QD emission, the CL-emission was recorded in  $\text{D}_2\text{O}$  as a solvent instead of  $\text{H}_2\text{O}$ , because  $^1\text{O}_2$  possesses a 13 times longer lifetime in  $\text{D}_2\text{O}$  than in  $\text{H}_2\text{O}$ .<sup>24</sup> Generally, if the CL emission originated from  $^1\text{O}_2$ , one would expect alteration of the kinetic reaction in  $\text{D}_2\text{O}$ . However, no obvious change was observed, indicating no contribution of the  $^1\text{O}_2$  to the CL-emission due to the annihilation of electron-hole combination of  $(\text{MoS}_2)^{+\bullet}$  QDs and  $(\text{MoS}_2)^{-\bullet}$  QDs (Fig. S8, ESI†).

## Conclusions

For the first time, we have demonstrated the excellent capability of  $\text{MoS}_2$ -QDs toward ROS generation. We explored that the synergistic effect of enhanced ROS production and ROS depletion were the main factors leading to the CL-emission of  $\text{MoS}_2$ -QDs with  $\text{H}_2\text{O}_2$  in alkaline medium; and with the Fenton reagent under neutral and acidic conditions. These findings present a new pathway for ROS generation over the whole pH-range. Thus,  $\text{MoS}_2$ -QDs have potential applications for degradation of organic pollutants and chemo-dynamic therapy.

## Conflicts of interest

There are no conflicts to declare.

## Acknowledgements

This work was supported by the National Natural Science Foundation of China (Nos. 21435002, 21621003) and JSPS RONPAKU (Ph.D. Dissertation) Program.

## References

- (a) H. Wang, S. Jiang, W. Shao, X. Zhang, S. Chen, X. Sun, Q. Zhang, Y. Luo and Y. Xie, *J. Am. Chem. Soc.*, 2018, **140**, 3474–3480; (b) R. C. Gilson, L. C. L. Black, D. D. Lane and S. Achilefu, *Angew. Chem., Int. Ed.*, 2017, **129**, 10857–10860; (c) J. Bai, X. D. Jia, W. Zhen, W. Cheng and X. Jiang, *Angew. Chem., Int. Ed.*, 2018, **140**, 106–109.
- (a) Y. Li, W. Zhang, J. F. Niu and Y. S. Chen, *ACS Nano*, 2012, **6**, 5164–5173; (b) C. Yang, W. Dong, G. Cui, Y. Zhao, X. Shi, X. Xia, B. Tang and W. Wang, *RSC Adv.*, 2017, **7**, 23699–23708; (c) Y. Zheng, D. Zhang, S. Shah, H. Li and J. Lin, *Chem. Commun.*, 2017, **53**, 5657–5660.
- (a) S. Shah, L. Lin, Y. Zheng, D. Zhang and J. Lin, *Phys. Chem. Chem. Phys.*, 2017, **19**, 21604–21611; (b) C. Zhang, W. Bu, D. Ni, S. Zhang, Q. Li, Z. Yao, J. Zhang, H. Yao, Z. Wang and J. Shi, *Angew. Chem., Int. Ed.*, 2016, **55**, 2101–2106.
- (a) O. Sanchez, D. Lembke, M. Kayci, A. Radenovic and A. Kis, *Nat. Nanotechnol.*, 2013, **8**, 497–501; (b) Y. Lin, D. Dumcenco, Y. Huang and K. Suenaga, *Nat. Nanotechnol.*, 2014, **9**, 391–396; (c) C. Zhu, Z. Zeng, H. Li, F. Li, C. Fan and H. Zhang, *J. Am. Chem. Soc.*, 2013, **135**, 5998–6001.
- (a) G. Li, D. Zhang, Y. Yu, S. Huang, W. Yang and L. Cao, *J. Am. Chem. Soc.*, 2017, **139**, 16194–16200; (b) Y. Shi, Y. Zhou, D. Yang, W. Xu, C. Wang, F. Wang, J. Xu, X. Xia and H. Chen, *J. Am. Chem. Soc.*, 2017, **139**, 15479–15485; (c) X. Zhao, H. Zhu and X. Yang, *Nanoscale*, 2014, **6**, 10680–10685.
- J. Wang, X. Tan, X. Pang, L. Liu, F. Tan and N. Li, *ACS Appl. Mater. Interfaces*, 2016, **8**, 24331–24338.
- O. Spalek, J. Balej and I. Pasek, *J. Chem. Soc., Faraday Trans. 1*, 1982, **78**, 2349–2359.
- A. Hebeish, A. Bayazeed, B. I. Abdel Gawad, S. K. Basily and S. El-Bazza, *Starch*, 1984, **10**, 344–349.
- Y. Ouyang, C. Ling, Q. Chen, Z. Wang, L. Shi and J. Wang, *Chem. Mater.*, 2016, **28**, 4390–4396.
- L. Kong, G. Fang, Y. Kong, M. Xie, V. Natarajan, D. Zhou and J. Zhan, *J. Hazard. Mater.*, 2018, **357**, 109–118.
- N. Zhou, T. Qiu, L. Ping and L. Yang, *Magn. Reson. Chem.*, 2006, **44**, 38–44.
- K. Reybier, S. Ayala, B. Alies, J. V. Rodrigues, S. B. Rodriguez, G. Penna, F. Collin, C. M. Gomes, C. Hureau and P. Faller, *Angew. Chem., Int. Ed.*, 2016, **55**, 1085–1089.
- Y. Zheng, X. Dou, H. Li and J.-M. Lin, *Nanoscale*, 2016, **8**, 4933–4937.
- I. Ivanova, S. Trofimova, I. Piskarev, N. Aristova, O. Burhina and O. Soshnikova, *J. Biophys. Chem.*, 2012, **3**, 88–100.
- Z. Lin, H. Chen, Y. n. Zhou, N. Ogawa and J.-M. Lin, *J. Environ. Sci.*, 2012, **24**, 550–557.
- W. Zhang, S. Hu, J. Yin, W. He, W. Lu, M. Ma, N. Gu and Y. Zhang, *J. Am. Chem. Soc.*, 2016, **138**, 5860–5865.
- W. Zhang, Y. Su, X. Zhang, Y. Yang and X. Guo, *RSC Adv.*, 2016, **6**, 64626–64633.
- E. Munaf, R. Zein, R. Kurniadi and I. Kurniadi, *Environ. Technol.*, 1997, **18**, 355–358.
- Y. Li, Y. Zheng, D. Zhang, H. Li, Y. Ma and J. M. Lin, *Chin. Chem. Lett.*, 2017, **28**, 184–188.
- G. Buxton, C. Greenstock, W. Helman and A. B. Ross, *J. Phys. Chem. Ref. Data*, 1988, **17**, 513–861.
- W. Haag and C. Yao, *Environ. Sci. Technol.*, 1992, **26**, 1005–1013.
- B. Chen, F. Wang, W. Yao, Z. Lin, X. Zhang, S. Luo, L. Zheng and X. Lin, *Anal. Methods*, 2018, **10**, 474–480.
- W. Adam, D. V. Kazakov and V. P. Kazakov, *Chem. Rev.*, 2005, **105**, 3371–3387.
- R. Huang, E. Choe and D. B. Min, *J. Food Sci.*, 2004, **69**, 726–732.

